Tight-Binding Computation of the STM Image of Carbon Nanotubes

V. Meunier* and Ph. Lambin
Département de Physique, Facultés Universitaires Notre-Dame de la Paix, 61 Rue de Bruxelles, B-5000 Namur, Belgium
(Received 6 October 1998)

STM imaging of single-wall carbon nanotubes has recently been achieved with atomic resolution, revealing the chirality of the carbon network. In this work, a theoretical modeling of scanning tunneling microscopy of the nanotubes is presented, based on a tight-binding π-electron Hamiltonian. This theory is simple enough to be used routinely for the computation of STM images and current-voltage characteristics, making it possible to investigate specific effects of the network curvature and topology such as a pentagon-heptagon pair defect. [S0031-9007(98)07951-4]

PACS numbers: 61.48.+c, 61.16.Ch, 68.35.Bs

The research on carbon nanotubes has attracted an increasing growth of interest in the recent years due to their quasi-one-dimensional structure [1]. Most of the properties of single-wall carbon nanotubes (SWNT's) are now well understood, at least for defect-free materials having a remarkably simple atomic structure. This structure is completely determined by the circumferential vector $\vec{c}_h = n\vec{a}_1 + m\vec{a}_2$ with components (n, m) along two Bravais primitive translations of a graphene sheet. The $\vec{c}_h$ vector in turn governs several properties dependent on the diameter (Young modulus [2], Raman spectrum [3], ...) and finely controls the electronic and magnetic properties of the nanotube [4–7].

Scanning tunneling microscopy (STM) is one among the very few experimental techniques available for determining the (n, m) indices of an isolated nanotube [8–10]. This is not easy, however, since it demands the atomic resolution. The indices are then deduced from two independent measurements [8,11]: The diameter of the nanotube ($|\vec{c}_h|/2\pi$) and the angle that a zigzag chain of atoms makes with the axis of the nanotube (pitch angle $\tan^{-1}[(n - m)/\sqrt{3}\,(n + m)]$). The diameter is difficult to measure with precision, because of tip-shape convolution effects and various electronic effects [12]. The angle of a zigzag direction can be affected by distortions induced by a torsional twist [13] and by the cylindrical structure of the nanotube itself, as shown below. All these difficulties show that a theoretical calculation of the STM image is highly desirable to check the validity of the interpretation. In this communication, it is shown that a simple tight-binding calculation of the tunneling current may prove to be useful for that purpose. Its validity has been confirmed recently by *ab initio* test calculations [14].

The starting point of the STM current calculation is the well-known expression

$$\mathcal{I} = \frac{2\pi e}{\hbar} \int dE[f_t(E) - f_s(E)] \times \sum_{\alpha,\beta} |\langle\alpha|v|\beta\rangle|^2 \delta(E - E_\alpha)\delta(E - E_\beta), \quad (1)$$

where $|\alpha\rangle$ and $|\beta\rangle$ are unperturbed electronic states of the tip (t) and sample (s), respectively, with energies E_α and E_β, f_t and f_s are the Fermi-Dirac distributions, and v is the coupling Hamiltonian between tip and sample. In tight binding, assuming one orbital per atom to simplify, one has

$$|\alpha\rangle = \sum_{I\in t} \chi_I^\alpha |\eta_I\rangle, \qquad |\beta\rangle = \sum_{J\in s} \psi_J^\beta |\theta_J\rangle, \quad (2)$$

where $|\eta_I\rangle$ and $|\theta_J\rangle$ are atomic orbitals on tip and sample sites, respectively, with χ_I^α and ψ_J^β the LCAO coefficients. Let $v_{IJ} = \langle\chi_I|v|\theta_J\rangle$ be the tight-binding tip-sample coupling elements and use [15]

$$\sum_{\beta\in s} \psi_J^{\beta*}\delta(E - E_\beta)\psi_{J'}^\beta = \frac{-1}{\pi}\,\mathrm{Im}\,R_{JJ'}^s(E + i0) \equiv n_{JJ'}^s(E), \quad (3)$$

valid with time reversal symmetry, where $R_{JJ'}^s$ is an element of the Green function of the sample (a similar expression is obtained on the tip side). The current at 0 K deduced from Eq. (1) is

$$\mathcal{I} = (2\pi)^2 \frac{e}{h} \int_{-eV}^{0} dE \sum_{I,I'\in t} \sum_{J,J'\in s} v_{IJ} v_{I'J'}^* \times n_{II'}^t(E_F^t + eV + E) n_{JJ'}^s(E_F^s + E), \quad (4)$$

where V is the tip-sample bias potential ($e > 0$), and the E_F's are the Fermi levels of the unperturbed systems. When deriving that equation, the one-electron energy levels of the tip were shifted rigidly to accommodate the contact potential $(E_F^t - E_F^s)/e$ and the bias potential V.

Ab initio calculations have shown that the substrate on which the nanotube is deposited plays only a small part in the STM image [14]. The nanotubes can therefore be considered as being self-supported. For all the applications illustrated below, the tip was described by a single atom with an s orbital, as in the Tersoff-Hamann theory [16]. The corresponding density of states $n^t(E)$ was assumed a Gaussian shape. The nanotube sample was described by a

 0031-9007/98/81(25)/5588(4)$15.00

π-electron tight-binding Hamiltonian with constant first-neighbor interactions ($\gamma_0 = -2.8$ eV). The corresponding diagonal and off-diagonal elements of the nanotube Green function $R^t_{JJ'}$ were calculated by recursion. The matrix elements coupling the tip apex atom to the atoms J of the nanotube were Slater-Koster sp like hopping interactions decaying exponentially with the separation distance d_J:

$$v_J = v_0 w_J e^{-d_J/\lambda} \cos\theta_J , \quad (5)$$

$$w_J = e^{-a d_J^2} / \sum_{J'} e^{-a d_{J'}^2} . \quad (6)$$

Here v_0 is an unimportant scaling factor (of the order of 1 eV), θ_J is the angle between the π-orbital lobe on site J and the local direction of the tip atom, and w_J is a weighting factor used to select the carbon atoms closest to the tip (within a disk of radius 2 Å centered on the projection of the tip apex on the nanotube). The parameters used were $\lambda = 0.85$ Å, $a = 0.6$ Å^{-2}. With these values, the tunneling current above a flat sheet of graphite decreases by a factor of 10 by increasing tip-sample distance by 1 Å. It has also been checked that the current asymmetry brought about by the unequivalence of the so-called A and B atoms in multilayered graphite comes out correctly from the calculations [17].

Figure 1 shows the derivative dI/dV of I-V curves computed for several nanotubes with diameter around 14 Å. These curves reflect the variations of the density of states of the nanotubes [diagonal terms $J = J'$ in Eq. (4)], affected by the convolution integral within the bias window, and distorted by the contribution of the off-diagonal elements $n^s_{JJ'}$. The latter, being nonsymmetric with respect to the Fermi energy, are responsible for the asymmetry of the differential conductance curves. As shown experimentally [9], the essential difference between the metallic and semiconducting nanotubes is the width of the small-conductance plateau around zero bias, which is about 1.7 V for the metals and 0.6 V for the semiconductors. The chirality of the structure does not contribute much to the curves [18].

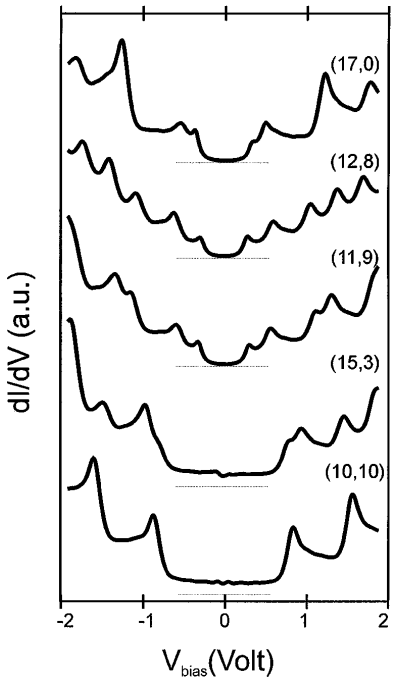

FIG. 1. Differential STM conductance when the tip is 5 Å above a sample atom for several nanotubes with equivalent diameters. The thin horizontal bars indicate zero conductance. (10,10) and (15,3) are metallic nanotubes; the others are semiconductors. The same units have been used for all the graphs.

In STM, a topographic image of a nanotube is represented against the coordinates (x, y) of the tip. Here, the nanotube is supposed to have its axis horizontal, along the x direction. At constant current, a moving pointlike tip remains roughly at constant height h from the nanotube. The tunneling current tends to follow the shortest path between tip and sample, i.e., to flow along the direction normal to the nanotube. Suppose there is an atom on the nanotube in this normal direction, at coordinates (x', y', z') (see Fig. 2). This atom is imaged by the tip when being at coordinates (x, y, z) given by $x = x'$, $y = y'\rho/R$, and $z = z'\rho/R$, where R is the nanotube radius and $\rho = R + h$ is the distance from the tip atom to the tube axis. In particular, there is an inflation of the distance by a factor of $1 + h/R$ along the transverse y direction.

The atomic corrugation of a nanoscopic object is generally hidden by its much larger geometrical corrugation which the tip must follow. The simplest way we found to subtract the cylindrical profile of the nanotube was to represent the axial distance ρ of the tip (or equivalently the distance h to the nanotube). On the topmost part of the tube, this is equivalent to representing the z coordinate of the tip, except for the lateral distortion mentioned above. We did not try to correct this distortion: maps of ρ at constant current were produced directly from Eq. (4) versus

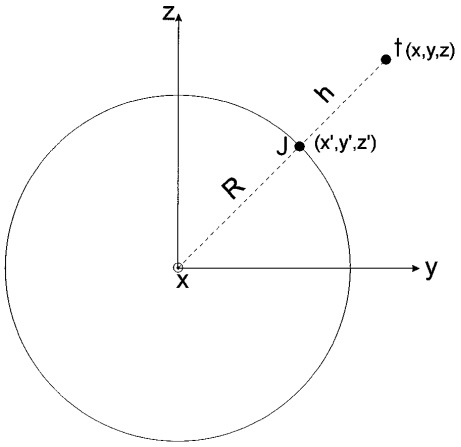

FIG. 2. When a pointlike tip t moves at constant distance h from a nanotube, the tunnel current through the atom J is at a maximum when t and J are aligned with the normal direction.

the tip atom x and y coordinates. We used the above relation between y and y' only to superpose the nanotube graphitic lattice onto the $\rho(x, y)$ maps, so as to identify the topographical features.

Figure 3 shows the $\rho(x, y)$ profile at constant current for four SWNT's of equivalent diameters. In all cases, the nanotube axis is along the horizontal direction (x), the topmost generator of the tubes coincides with the horizontal median ($y = 0$) of the rectangular maps. The height of the tip above the central atom is 5 Å. The atomic corrugation is the smallest (0.7 Å) for the (17,0) zigzag nanotube and reaches 1 Å with the (10,10) armchair structure. The centers of the honeycomb hexagons appear as sharp dips, which is confirmed by *ab initio* calculations [14], validating thereby the interpretation of the experimental observations [8–10,13]. This is also what is found in graphite [17]. The hexagon holes of the nanotubes are elongated along the vertical (y) direction due to the geometrical distortion discussed above. A consequence of the distortion is that the apparent angle of a zigzag chain of atoms with respect to the tube axis is overestimated, roughly by a factor of $1 + h/R$: 11° for (12,8) (instead of 6.6°) and 43° for (17,0) (instead of 30°). Whereas the atoms all look the same in the $\rho(x, y)$ profile of a single-wall nanotube, the bonds are not. In (17,0), for instance, the bonds parallel to the axis protrude more than the others. This characteristic changes with the chirality of the nanotube.

Signatures of pentagons have already been detected in scanning tunneling spectroscopy near the ending cap of multiwall nanotubes [19]. By contrast, a direct proof of the so-called pentagon-heptagon (5-7) defect, although probably a current feature [20], has never been clearly established. To help in the identification of such a defect, Fig. 4 shows STM images computed for a hybrid system made of connected (12,0) and (11,0) nanotubes. The connection between them is made possible by the presence of a pair of adjacent pentagon and heptagon aligned parallel to the axis [21]. The STM images in Fig. 4 are 3-dimensional representations of the tip vertical position $z(x, y)$ at constant current for two opposite bias potentials. The (11,0) nanotube is on the right, with its topmost generator 0.8 Å below that of (12,0). This difference in height (diameter) is represented by gray scale variations in the figure. The shape suggesting an arrowhead at the center is made by the bonds of the 5-7 defect lying on the top part of the structure. This arrowhead is a characteristic feature of the adjacent pentagon-heptagon defect. The two shallow dips on the right-hand side of the edge shared by the two odd-membered rings is the consequence of the boat-shaped form of the heptagon. The density of states of the (11,0) semiconductor is weakly affected by the 5-7 defect: its STM images look the same for two opposite bias potentials. One easily recognizes there the elongated shapes

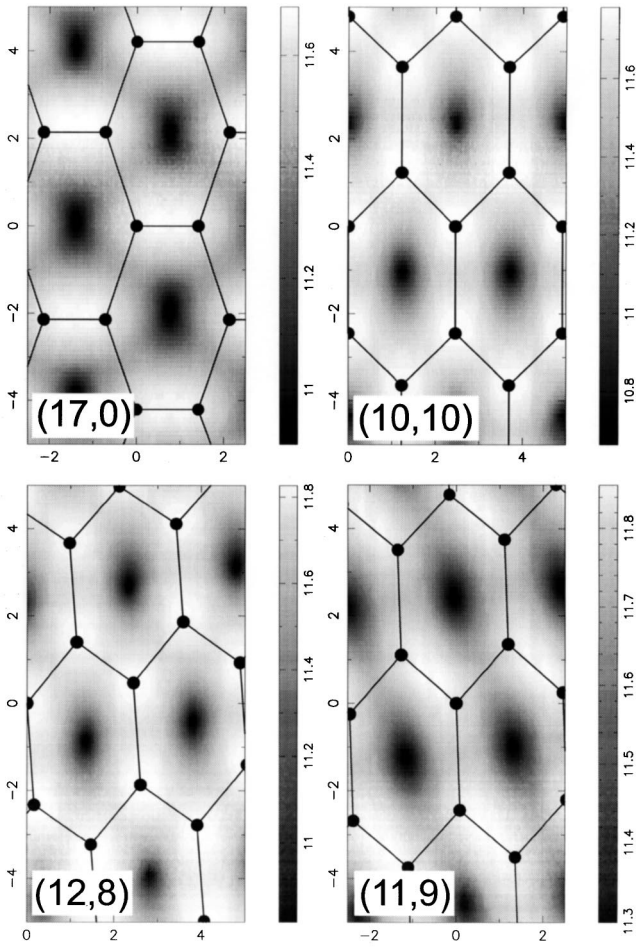

FIG. 3. Topographical STM images $\rho(x, y)$ at constant current for four nanotubes with equivalent diameters. In both cases, the horizontal direction is parallel to the nanotube axis. The tip potential is −0.5 V. The distorted graphitic lattice is visualized by black lines and black circles.

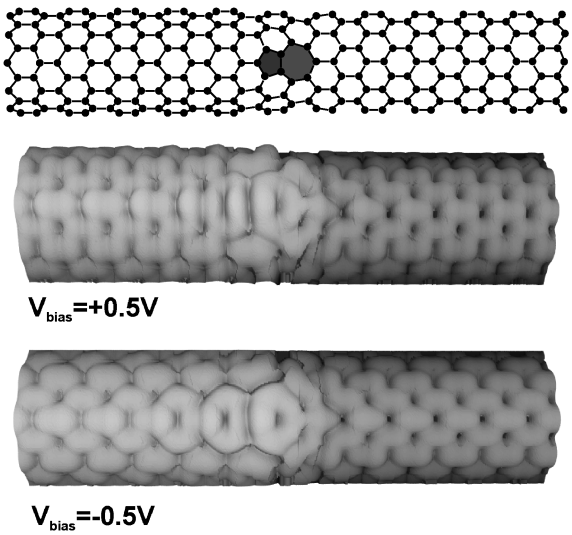

FIG. 4. Top: Atomic structure of the (12,0)/(11,0) connection with its 5-7 defect (shaded). Bottom: 3D representation of the STM tip height $z(x, y)$ at constant current for the same junction at +0.5 and −0.5 V bias voltages. The horizontal x dimension fits that of the atomic model.

of the hexagonal holes, separated from each other by the protruding C-C bonds parallel to the axis. On the metallic (12,0) side, the density of states is much more affected by the defect. As a consequence of the perturbation, the C atoms close to the pentagon are no longer equivalent; a dip appears near the center of the bonds parallel to the axis, which gradually fills in by moving away from the defect restoring progressively the STM topography of the unperturbed nanotube.

In summary, the best way to control the measurement of the diameter of an isolated SWNT is probably by measuring the width of the small conductance gap of the I-V curve (Fig. 1) at several places of the nanotube, and fitting the diameter from the $1/d$ law appropriate to the metallic or semiconducting case. Experimental STM images with atomic resolution are probably affected by a geometrical distortion of the kind illustrated in Fig. 2. This distortion stretches the graphitic lattice in the direction normal to the axis, and influences the measured chiral angle (Fig. 3). Geometrical or topographical defects (Fig. 4) have typical signatures in STM that, once cataloged, might allow their identification. The simple tight-binding model presented above makes this inventory feasible.

The authors acknowledge C. Dekker, A. Rubio, P. Senet, F. Marchal, F. Wiame, and J.-P. Vigneron for helpful discussions. This work has been partly funded by the Belgian Interuniversity Research Project on Reduced Dimensionality Systems (PAI-IUAP P4-10). V. M. acknowledges the FRIA organization for financial support.

*Electronic address: Vincent.Meunier@fundp.ac.be

[1] C. Journet and P. Bernier, Appl. Phys. A **67**, 1 (1998); Ch. M. Lieber, Solid State Commun. **107**, 607 (1998).
[2] E. Hernandez *et al.*, Phys. Rev. Lett. **80**, 4502 (1998).
[3] A. M. Rao *et al.*, Science **275**, 187 (1997).
[4] N. Hamada, S. I. Sawada, and A. Oshiyama, Phys. Rev. Lett. **68**, 1579 (1992).
[5] R. Saito *et al.*, Appl. Phys. Lett. **60**, 2204 (1992).
[6] H. Yorikawa and S. Muramatsu, Phys. Rev. B **52**, 2723 (1995).
[7] J. P. Lu, Phys. Rev. Lett. **74**, 1123 (1995).
[8] N. Lin *et al.*, Carbon **34**, 1295 (1996).
[9] J. W. G. Wildoer *et al.*, Nature (London) **391**, 59 (1998).
[10] T. W. Odom *et al.*, Nature (London) **391**, 62 (1998).
[11] L. C. Venema *et al.*, Appl. Phys. A **66**, S153 (1998).
[12] G. I. Márk, L. P. Biró, and J. Gyulai, Phys. Rev. B **58**, 12 645 (1998).
[13] W. Clauss, D. J. Bergeron, and A. T. Johnson, Phys. Rev. B **58**, R4266 (1998).
[14] A. Rubio *et al.*, "Electronic States in a Finite Carbon Nanotube: A One-Dimensional Quantum Box" (to be published).
[15] M. Tsukada and N. Shima, J. Phys. Soc. Jpn. **56**, 2875 (1987).
[16] J. Tersoff and D. R. Hamann, Phys. Rev. Lett. **50**, 1998 (1983).
[17] D. Tománek and S. G. Louie, Phys. Rev. B **37**, 8327 (1988).
[18] C. T. White and J. W. Mintmire, Nature (London) **394**, 29 (1998); J. C. Charlier and Ph. Lambin, Phys. Rev. B **57**, R15 037 (1998).
[19] D. L. Carroll *et al.*, Phys. Rev. Lett. **78**, 2811 (1997).
[20] S. Iijima, P. M. Ajayan, and T. Ichihashi, Phys. Rev. Lett. **69**, 3100 (1992).
[21] J. C. Charlier, T. W. Ebbesen, and Ph. Lambin, Phys. Rev. B **53**, 11 108 (1996).